

Novel Slow Dynamics of Phase Transition in the Partially Ordered Frustrated Magnet DyRu_2Si_2

Subaru Yoshimoto, Yoshikazu Tabata, Takeshi Waki, and Hiroyuki Nakamura
Department of Materials Science and Engineering, Kyoto University, Kyoto 606-8501, Japan

Abstract

DyRu_2Si_2 is a frustrated magnet exhibiting multiple magnetic phase transition in zero and finite magnetic fields. We investigated and characterized the phase transition between the partially-ordered antiferromagnetic phases at zero field by ac susceptibility measurements. Detailed ac susceptibility measurements reveal the novel critical dynamics of the phase transition; extremely slow dynamics with the relaxation time in the order of 10-100 ms, speed-up of the dynamics on cooling indicating its non-thermally activated origin and growing of the ferromagnetic correlations towards the phase transition temperature. On the basis of these findings, we propose a novel phase transition process, namely, the spontaneous striped-arrangement of the precedently emergent “belt-like” ferromagnetic spin textures.

1 Introduction

Frustrated magnets have been widely investigated for their rich variety of properties. In a frustrated system, where interactions compete, a vast number of physical states having the same energy co-exist and, therefore, the system is highly degenerated. These frustrated systems, such as spin glass and spin ice, are known to exhibit slow and complicated dynamics at low temperature because of their high degeneracy[1, 7, 2, 3, 4, 5, 6].

In the present report, we focus on the novel slow dynamics in the frustrated magnet DyRu_2Si_2 . It is one of the series of the intermetallic compound RT_2X_2 (R = rare earth, T = 4d or 5d metal, X = Si or Ge), with the tetragonal ThCr_2Si_2 -type structure, which exhibits a diversity of magnetic properties such as ferromagnetism, antiferromagnetism and paramagnetic heavy fermion [10, 8, 9]. The magnetic properties of RT_2X_2 are controlled by the interaction between the conduction electrons and f-electrons. In the heavy rare earth compounds, the f-electrons have strongly localized nature and complicated frustrated

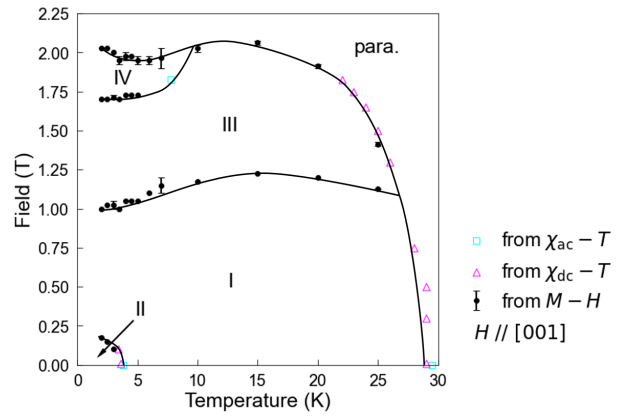


Figure 1: (Color online) H - T phase diagram of DyRu_2Si_2 . This phase diagram was reported in the literature[12] and confirmed in the present study.

magnetism is observed[11, 10] due to the frustration effect of the oscillating long-range RKKY interaction.

Among them, DyRu_2Si_2 is a representative frustrated RT_2X_2 , where magnetic Dy^{3+} ions have a strong c -axis anisotropy[12]. It exhibits multistep phase transition against temperature and magnetic field and has a complicated H - T phase diagram as shown in Fig. 1, which has paramagnetic and four antiferromagnetic phases. Kawano et al. have revealed the magnetic structure of each phase from the results of neutron scattering[13]. In zero magnetic field, it was indicated that the phase I and II are partially antiferromagnetically ordered phases, where fluctuating spins still remain even below their transition temperatures. The magnetic structures of these phases, which are extensively investigated in this study, are schematically shown in Figs. 2 (a) and (b). The phase I has a stripe structure which has a long period along the a -axis with the propagation vector $Q = (2/9, 0, 0)$ [13]. Considering the

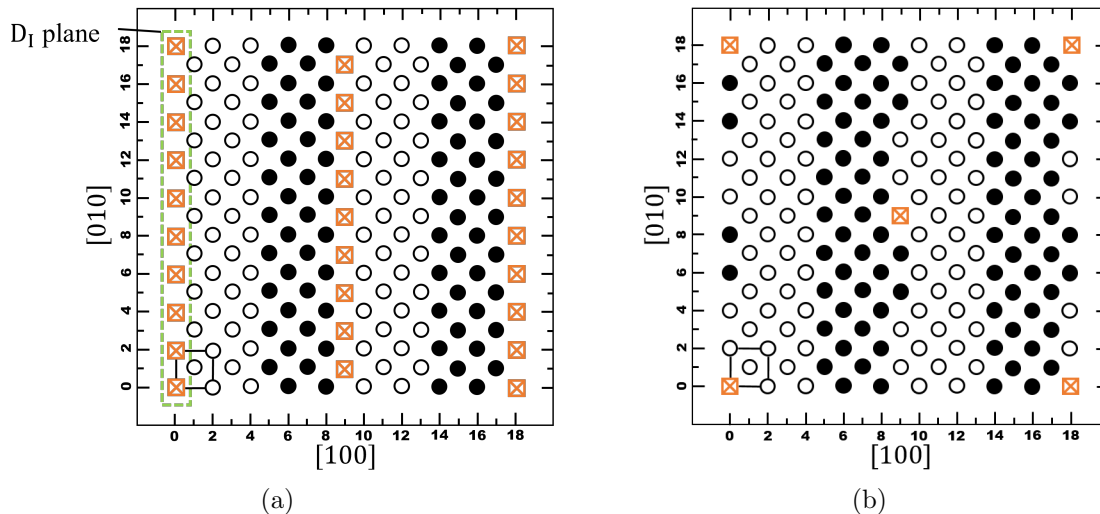


Figure 2: (Color online) Schematic views of the magnetic structures projected on the basal c-plane of (a) the phase I and (b) II of DyRu_2Si_2 . A square on the left bottom of each figure represents the crystallographic unit cell and each circle or square represents a Dy ion on the corner or body-centered position. The unit of axes is half a lattice constant $a/2$. The open and closed circles indicate the Dy ions with the spins parallel and antiparallel to the c -axis, respectively. The orange square with a cross represents the Dy ion with the fluctuating spin.

C_4 symmetry of the crystal structure, one expects the formation of two equivalent domains A and B, which have the period along the a - and b -axes, respectively. However, the magnetic responses of two domains against the magnetic field along the c -axis are indistinguishable, and thus all description hereafter is based on only the A-domain for simplicity. It is noteworthy that disordered paramagnetic a -planes (denoted as the D_I planes hereafter) appear every 9 ordered a -planes. It is indicated that the spins in the D_I plane are magnetically free, namely, interactions from the neighboring and further ordered a -planes compete with each other and are canceled out. Thus, these spins on the D_I planes can be considered as a pseudo two-dimensional system. The phase II has the magnetic structure where the spins in the D_I planes are partly ordered along the b -axis. Such partially ordered states due to the insufficient lift of the degeneracy are also found in other frustrated magnets [15, 14, 18, 17, 19, 16, 20, 21]. In these systems, slow spin dynamics owing to the paramagnetic, but strongly correlated, fragment is often observed[22]. Thus, from the magnetic structures of the partially ordered phases I and II, one can expect novel slow dynamics in this DyRu_2Si_2 due to the fluctuating spins.

In the present study, we have performed de-

tailed ac-susceptibility measurements to reveal it and have found novel critical dynamics accompanying the phase transition between these partially ordered phases I and II. The striking features of the novel dynamics are the following three points. First, its relaxation time is extremely long (order of 10-100 ms). Second, the dynamics becomes faster on cooling indicating non-thermally activated origin. Third, ferromagnetic correlations grow towards the phase transition temperature even though both phases are antiferromagnetic. Of course, in spin glass or spin ice, slow dynamics with the relaxation time of s-ms order is often observed[1, 7]. In such a system, it can be attributed to the glassy nature due to the high degeneracy at low temperature. However, since this is not the case in DyRu_2Si_2 , it is an intriguing outcome that we observed such a long relaxation time over the I-II phase transition. On the basis of these findings, we proposed the process of the phase transition, namely, the spontaneous stripe-arrangement of the precedently emergent “belt-like” ferromagnetic spin textures.

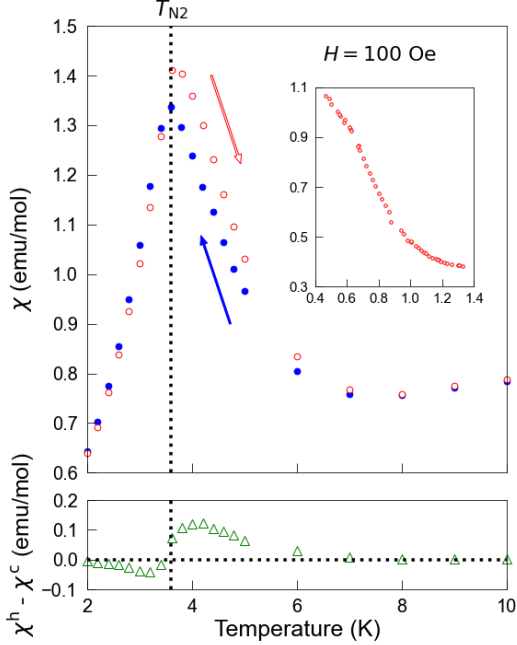


Figure 3: (Color online) Temperature hysteresis of the dc susceptibility over the I-II phase transition. χ^h and χ^c are denoted as red-open and blue-closed circles, respectively. Green-open triangles represent the difference of χ^h and χ^c . The inset shows the susceptibility in the temperature region below the I-II phase transition. The measurement protocols are described in the text.

2 Experimental Details

We synthesized a polycrystalline sample with an arc furnace followed by single crystal growth by the Czochralski pulling method with a tetra arc furnace. The grown single crystal was cut, and finally, a cubic-like-shaped sample with the weight of 10.1 mg was obtained for dc and ac susceptibility measurements. We performed dc and ac susceptibility measurements using the SQUID magnetometer (MPMS, Quantum Design) equipped in the Research Center for Low Temperature and Materials Sciences, Kyoto University. Firstly, the magnetic field dependences of magnetization at several temperatures and the temperature dependences of the dc and ac susceptibilities at several magnetic fields were examined to confirm the H - T phase diagram of DyRu_2Si_2 in the literature[12]. The result is denoted in Fig. 1. Also, we measured detailed frequency dependences of ac susceptibility in the vicinity of the I-II phase transition temperature at zero bias field for revealing the critical dynamics and at $H = 5$ kOe for a comparison. The ac susceptibility measurements were performed with the ampli-

tude of the oscillating field of 3 Oe and the frequency region of 0.1-1000 Hz.

3 Results

The temperature dependences of the dc susceptibility over the I-II phase transition at 100 Oe in the cooling and heating processes are shown in Fig. 3. On the measurement, we first cooled down to 10 K under zero-field-cooled (ZFC) condition and set magnetic field of 100 Oe. Then we measured magnetization on cooling down to 1.8 K and went backward. Let χ^h , χ^c and T_{N2} be the susceptibilities measured on heating and on cooling and the transition temperature of the I-II phase transition, respectively. The temperature dependences of χ^h and χ^c are roughly similar. The peak temperature of χ^h and χ^c , which are the sign of the phase transition, are the same. Although, since there is the hysteresis behavior, the phase transition temperature T_{N2} cannot be accurately identified, it is approximately evaluated as 3.6 K. This corresponds to the phase transition temperature reported in the earlier work[12]. As shown in the lower panel of Fig. 3, the magnitude of χ^h is greater than that of χ^c in the temperature region of $T \geq T_{N2}$ and, vice versa, $\chi^c > \chi^h$ for $T < T_{N2}$. The hysteresis behavior of the dc susceptibility indicates the presence of slow dynamics accompanying the I-II phase transition in the time scale of the measurement or longer and was not observed over the para-I phase transition (not shown).

The inset of Fig. 3 shows the lower temperature susceptibility below T_{N2} . The measurement was performed with the heating process after ZFC down to 0.46 K and applying magnetic field of 100 Oe. Here, it is found that the susceptibility increases down to the lowest measured temperature 0.46 K, which indicates the presence of the fluctuating Dy spins in the phase II (Fig. 2 (b)) and its persistence down to this temperature. This result is consistent with the increase of the specific heat towards the lowest temperature in the phase II, reported in the previous study[12]. We are not sure whether there is temperature hysteresis in this temperature region as well as above 1.8 K and whether there is another phase transition, where the fluctuating spins order, at lower temperature. It will be investigated in the near future.

Figures 4 (a) and (b) are the temperature dependences of the ac susceptibility, the real part χ' and imaginary part χ'' at the bias field of 0 and 5 kOe. At zero field (Fig. 4 (a)), two-step phase transition at $T_{N1} = 29.5$ K and at T_{N2} , corresponding to the para-I and I-II phase transitions respectively, are clearly seen. Here T_{N1} is the phase transition temperature of the para-I phase transition. In the plot of the real part

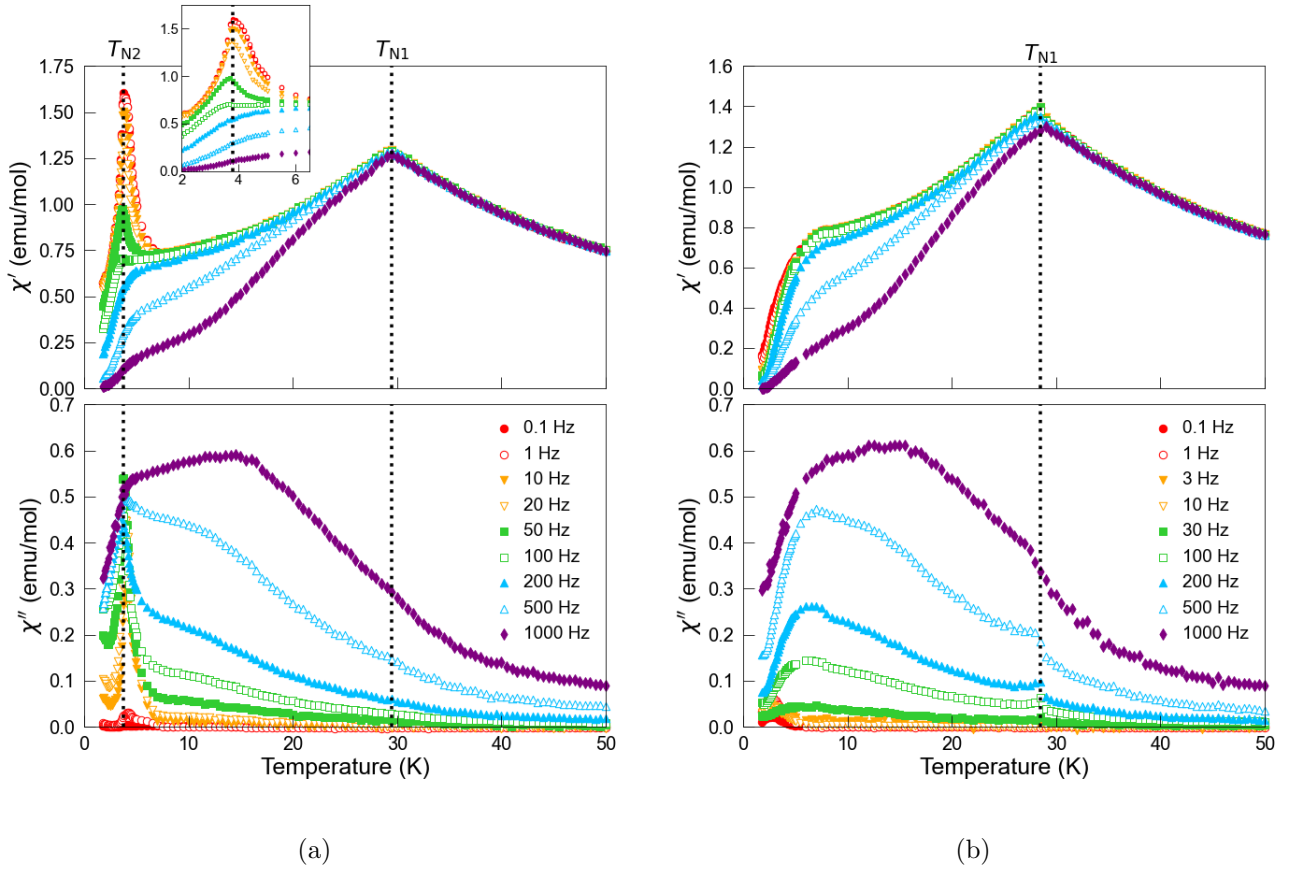


Figure 4: (Color online) Temperature dependences of the real (upper) and imaginary (bottom) parts of the ac susceptibility at the bias field of (a) 0 and (b) 5 kOe. The inset of the upper figure in (a) is the enlarged figure of the low-temperature region. Both temperature dependences were measured with elevating temperature after ZFC.

χ' at zero field, the peak temperature corresponding to the I-II phase transition is 3.8 K, which is slightly different from 3.6 K of the peak temperature in the dc susceptibility. This difference should come from the non-equilibrium effect in the vicinity of T_{N2} . The transition temperature should ideally be unique and thus we have to say that the true transition temperature is not able to be identified but some value around 3.6 K. In zero field, there is no frequency dependence of χ' in the paramagnetic phase and in the vicinity of the para-I phase transition, whereas strong frequency dependence of χ' and corresponding substantial χ'' appear especially above 100 Hz in the phase I and II. It is remarkable that the striking frequency dependence of χ' in the lower frequency region is found in the vicinity of T_{N2} , where the peak attenuates with increasing frequency and disappears above 100 Hz. Correspondingly, a sharp peak of χ'' and its suppression with increasing frequency are observed at T_{N2} .

At $H = 5$ kOe (Fig. 4 (b)), similar behavior of both χ' and χ'' are seen in the paramagnetic phase and phase I, whereas, the peak anomalies of χ' and χ'' attributed to the I-II phase transition are absent. These results indicate the presence of slow dynamics in the phase I and II with long relaxation times of the order of 10 ms. This feature should be attributed to the fluctuating spins in each partially ordered phase. The slower dynamics in the vicinity of T_{N2} is more striking and should be associated with the characteristic hysteresis behavior of the dc susceptibility.

In order to investigate the slow dynamics attributed to the I-II phase transition more deeply, we measured more detailed frequency dependences of the ac susceptibility between the temperature of 3.0 K and 6.0 K at zero field. Since the I-II phase transition shows the temperature hysteresis, we measured the frequency dependences on both cooling and heating. The frequency dependences measured on cooling are shown

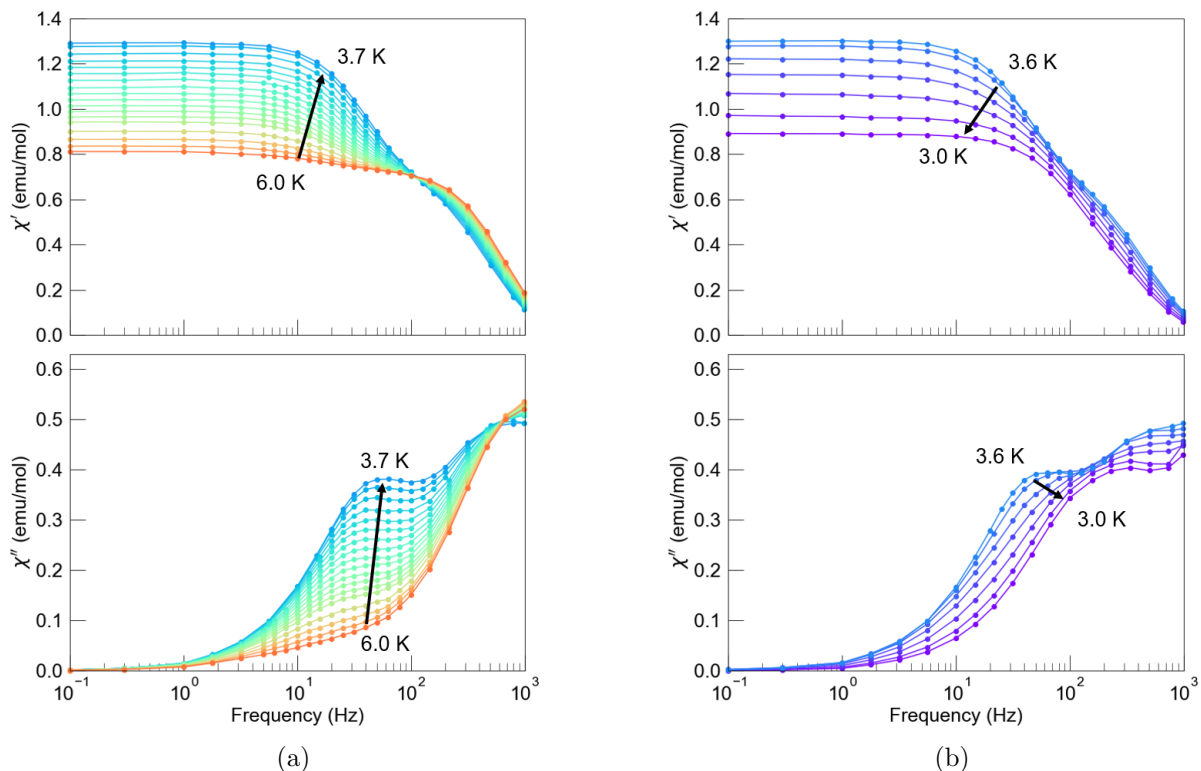


Figure 5: (Color online) Frequency dependences of the real (upper) and imaginary (lower) parts of the ac susceptibility (a) above 3.7 K and (b) below 3.6 K at zero field measured on cooling.

in Figs. 5 (a) and (b), which show the plots of the temperature range above 3.7 K and below 3.6 K, respectively. In Fig. 5 (a), the real part χ' at 6.0 K shows a one-step-like structure which has a reduction at around 200 Hz and it changes to a two-step-like structure, where another reduction at around 10 Hz appears, with approaching T_{N2} . In Fig. 5 (b), it changes to a one-step-like one again with decreasing temperature further. One can see the feature of the change of dynamics more clearly in the imaginary part χ'' . At 6.0 K in Fig. 5 (a), it shows a one-peak-like structure with a peak around 1000 Hz, or higher, corresponding to the one-step-like structure of χ' at 6.0 K. With decreasing temperature, an additional peak appears around 10 Hz. This peak shifts to a higher frequency with approaching T_{N2} . In Fig. 5 (b), it merges into the higher frequency peak further below T_{N2} . These changes of χ'' correspond to the development of the two-step-like structure and the retransformation to the one-step-like one in χ' . These results indicate that the system has several relaxation components owing to the phases I and II themselves and the I-II phase transition. It is noteworthy that

the characteristic frequency, owing to the I-II phase transition that gives the reduction of χ' and the peak of χ'' observed below 6.0 K, increases with decreasing temperature. The frequency dependences of the ac susceptibility measured on heating exhibits similar behavior, but is greater in magnitude.

4 Analysis

The I-II phase transition at T_{N2} in DyRu_2Si_2 is noteworthy in three points. First, it has the characteristic temperature hysteresis. Second, it is accompanied by extremely slow dynamics, where the peak anomaly at T_{N2} has a significant frequency dependence and it attenuates with increasing frequency. Third, the characteristic frequency of the “critical dynamics” of the I-II phase transition increases with decreasing temperature, which implies a non-thermally activated origin.

For further discussion on the dynamics of the I-II phase transition, we subtracted the “background” dynamics owing to the phase I, which is observed in the high-frequency range. As seen in the H - T phase dia-

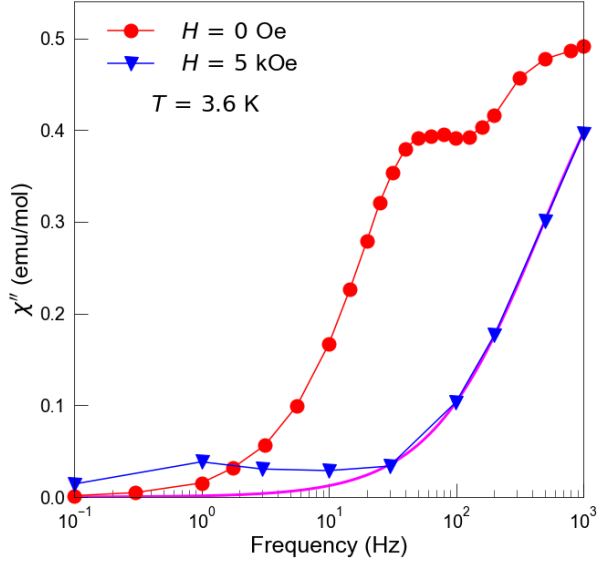


Figure 6: (Color online) Comparison of the frequency dependences of χ'' in the field of 0 and 5 kOe at 3.6 K in the cooling process. The pink solid curve is the fitting curve (see the main text).

gram in Fig. 1, the phase II appears in the low-field region. We, therefore, assumed that the frequency dependence of the ac susceptibility at $H = 5$ kOe, which characterizes the dynamics of the phase I, is the background. Figure 6 shows the comparison of the frequency dependences of χ'' at zero field measured on the cooling process and χ'' at 5 kOe. It indicates that χ'' at $H = 5$ kOe is appropriate to be assumed as the background, except for the low-frequency region, where a small broad peak around 1 Hz was observed. For the subtraction, first, we neglected the small peak. This is because the peak is considered to originate from the dynamics of the process where the fluctuating spins in the D_I plane are getting aligned to the magnetic field direction as lowering temperature, and such dynamics should be absent at zero magnetic field. Thus, as depicted by the pink solid curve in the figure, we presumed the fitting result using χ'' of the high frequency region above 20 Hz at $H = 5$ kOe to be the background in the full frequency range. The fitting function is $\chi''_{bg}(\omega) = \chi_{bg} \omega \tau_{bg} / \{1 + (\omega \tau_{bg})^\alpha\}$, where ω is the frequency and χ_{bg} , τ_{bg} and α are fitting parameters. This function describes the high-frequency χ'' at $H = 5$ kOe well, even though it is an ad hoc function and lacks clear physical meaning.

Figure 7 shows the frequency dependence of χ'' at 3.6 K after the background-subtraction. Hereafter let

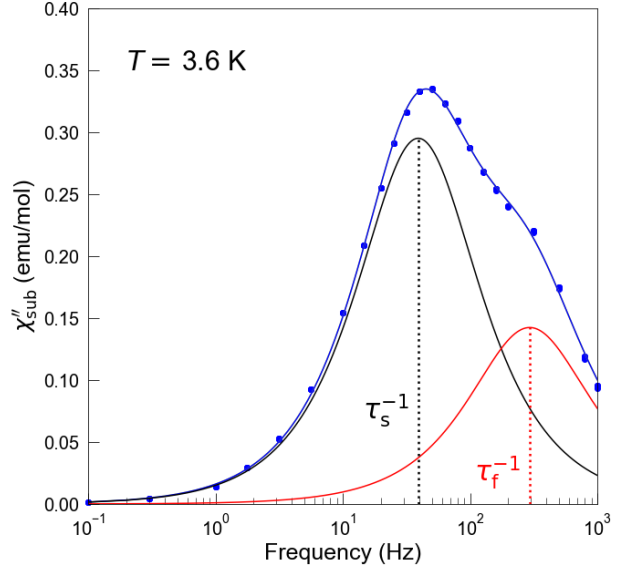


Figure 7: (Color online) Frequency dependence of χ''_{sub} at 3.6 K and the fitting results by the double Debye relaxation (the blue curve). The black and red curves indicate the slower and faster terms, respectively.

this subtracted susceptibility by χ''_{sub} . It has two peak structures around 40 Hz and 300 Hz. The frequency dependence of χ''_{sub} is well described by double Debye relaxation;

$$\chi''_{sub} = \chi_s \frac{\omega \tau_s}{1 + (\omega \tau_s)^2} + \chi_f \frac{\omega \tau_f}{1 + (\omega \tau_f)^2}, \quad (1)$$

where $\chi_{s,f}$ and $\tau_{s,f}$ are the isothermal susceptibilities and relaxation times, and the subscripts “s” and “f” denote the slower and faster terms with longer and shorter relaxation times, respectively.

The temperature variation of the frequency dependence of χ''_{sub} in the cooling process is shown in the upper panel of Fig. 8. Both peaks emerge at 6.0 K, and grow up on cooling. The slower term in the lower frequency region increases towards T_{N2} and exhibits maximum with slight shifting towards higher frequency. On the other hand, the faster one keeps on growing on further cooling. χ''_{sub} in the heating process was also derived by the same procedure, shown in the lower panel of Fig. 8. It is also able to be fit by the double Debye relaxation and shows the similar temperature variation.

Figures 9 (a) and (b) are the temperature dependences of the parameters, isothermal susceptibilities and relaxation times, respectively. The superscripts

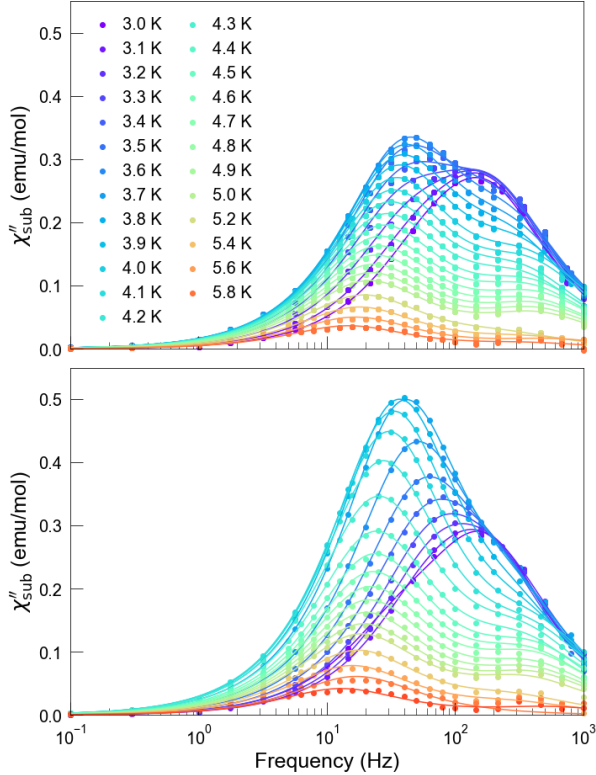


Figure 8: (Color online) Frequency dependences of χ''_{sub} at various temperatures in the cooling (upper) and heating (lower) processes. The solid lines are the fitting results of the double Debye relaxation.

of “h” and “c” denote the parameters in the heating and cooling processes, respectively. In Fig. 9 (a), the isothermal susceptibility of the slower term χ_s exhibits clear peak and hysteresis around $T_{\text{N}2}$. χ_s^c and χ_s^h show the peaks at slightly different temperatures, $T_{\text{peak}}^c = 3.6$ K and $T_{\text{peak}}^h = 3.8$ K, and the peak in the heating process is more pronounced. χ_s^c and χ_s^h merge far above $T_{\text{N}2}$ ($T > 5.6$ K) and below $T_{\text{N}2}$ ($T < 3.2$ K). In the figure, we also plot the real part of the ac susceptibility at the lowest frequency, 0.1 Hz, χ_0^c and χ_0^h measured on both the cooling and heating processes. They behave similarly to $\chi_s^{c,h}$ around $T_{\text{N}2}$. Note that we didn’t subtract the background from these susceptibilities $\chi_0^{c,h}$. Thus, it can be concluded that the characteristic features in χ_s^c and χ_s^h are not artifacts owing to the background-subtraction or the phenomenological fitting by the double Debye relaxation. In contrast to the slower term, the isothermal susceptibilities of the faster terms, χ_f^c and χ_f^h , do not exhibit remarkable hysteresis behaviors and any anomalies around $T_{\text{N}2}$.

The both χ_f moderately increase down to the lower temperature than $T_{\text{N}2}$. It should be noted that this is consistent with the increase of the dc susceptibility on cooling down to 0.46 K as shown in the inset of Fig. 3. The difference between the temperature dependences of χ_s and χ_f obviously indicates that the slower and faster terms of χ''_{sub} are attributed to different dynamics: the critical dynamics of the I-II phase transition and the dynamics of the disordered spins in the phase II, respectively.

Figure 9 (b) shows the temperature dependences of the relaxation times of the slower and faster components, τ_s and τ_f . The relaxation time τ_s , which is attributed to the dynamics of I-II phase transition, reveals two noteworthy facts about it. First, the relaxation time is extremely long. At around 5.8 K, it is in the order of 100 ms and it declines almost linearly towards $T_{\text{N}2}$. Second, it is indicated that the dynamics of the I-II phase transition is non-thermally activated, because the relaxation time decreases with temperature decreasing. This is consistent with the temperature variation of χ''_{sub} shown in Fig. 8 and it is more apparent here. It should be also noted that the critical slowing down towards $T_{\text{N}2}$ is absent. As seen in the isothermal susceptibility χ_s , the relaxation time τ_s also shows the hysteresis behavior, especially below $T_{\text{N}2}$. The relaxation time in the cooling process τ_s^c shows a hump at around 3.4 K. On the other hand, that in the heating process τ_s^h shows a minimum at around 3.2 K and is smaller than τ_s^c . Above $T_{\text{N}2}$, the size relationship between τ_s^c and τ_s^h is reversed, namely, τ_s^h is slightly larger than τ_s^c . In contrast to τ_s , the relaxation time of the faster term τ_f doesn’t show significant hysteresis behavior and increases moderately with temperature decreasing below T_{peak}^c . It indicates that the faster dynamics is thermally activated. Again, these differences between τ_s and τ_f indicate the different origins of the two dynamics.

Figure 9 (c) shows the temperature dependences of products of the isothermal susceptibility and temperature $T\chi_s$ for the two processes, which corresponds to the spin correlations;

$$T\chi_s \propto \sum_{i,j} \langle S_i S_j \rangle. \quad (2)$$

This quantity increases when ferromagnetic (FM) spin correlations develop, whereas, decreases when antiferromagnetic (AFM) spin correlations develop. The I-II phase transition is the process where the spins in the disordered D_I plane form the striped AFM order along the b-axis. Nevertheless, $T\chi_s^{c,h}$ increase towards $T_{\text{N}2}$, which indicates that growth of dynamic FM correlations is involved in the phase transition. It might look contradictory, however, as

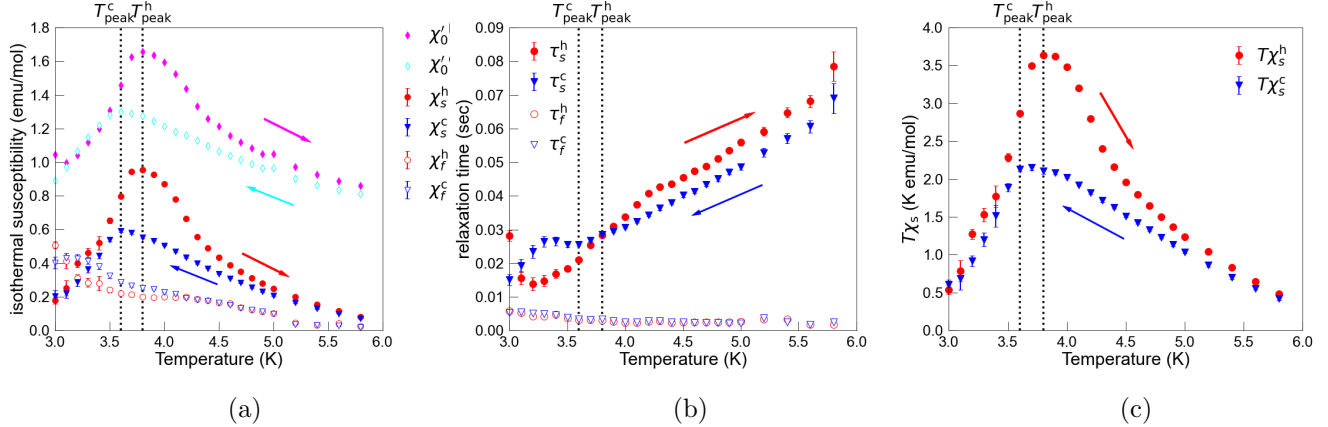


Figure 9: (Color online) Temperature dependences of the fitting parameters of χ''_{sub} by the double Debye relaxation: (a) the isothermal susceptibilities χ_s and χ_f , and (b) relaxation times τ_s and τ_f . The real part of the ac susceptibility at 0.1 Hz, χ'_0 , is also plotted in (a). (c) $T\chi_s$ as the function of temperature. Superscripts of “h” and “c” denote the heating and cooling processes, respectively. Arrows in the figures represent the directions of the measurement processes.

discussed in Sec. 5, it indicates important information about this extraordinary phase transition.

5 Discussion

In this section, we propose the process of the I-II phase transition indicated by the above analysis.

As a summary of the analysis, the features of the dynamics attributed to the I-II phase transition are the following;

1. Dynamic FM correlations with long relaxation time appear at around 6 K and grow towards the I-II phase transition temperature T_{N2} ,
2. The dynamics is non-thermally activated,
3. The dynamics shows hysteresis behavior as shown in the temperature dependences of χ_s and τ_s (Figs. 9 (a) and (b)).

The feature (1) indicates that large dynamic FM spin textures appear precedently to the phase transition. In general, the response time of a spin system is in the order of ps-ns. Thus, the observed long relaxation time indicates that the spin textures should be considerably large. Since the I-II phase transition is the process where the fluctuating spins in the D_I planes form the striped order of the phase II, it is reasonable to consider that the FM spin textures appear and grow in the D_I plane and they are strongly involved with the development of the striped spin correlations.

On the basis of these considerations, we propose a schematic picture of the I-II phase transition as

shown in Fig. 10, where the development and shift of spin correlations with temperature variation in the D_I plane, which is represented by the column of the orange cross-squares surrounded by the green dashed rectangle in Fig. 2, are shown. All the panels show the projection onto the a-plane. The striped pattern of the phase II in Fig. 10 indicates that the nearest-neighbor (NN) interaction is FM along both the b- and c-axes and the AFM next-nearest-neighbor (NNN), and maybe further long-range interactions, compete with the NN FM interaction along the b-axis, whereas, further interactions are too weak to compete with the NN FM interactions along the c-axis. Thus, we hypothesize that the non-frustrated two-row FM spin textures are formable at much higher temperature than the phase transition temperature and the large “belt-like” FM correlated spin textures emerge around 6 K as precursors of the striped AFM structure of the phase II, as shown in the right panel of Fig. 10. Then, they grow larger and become denser with decreasing temperature, and finally spontaneously form the striped magnetic structure at T_{N2} as shown in the left panel of Fig. 10.

The non-thermally activated behavior of the relaxation time τ_s can be explained in this picture as follows. The key of the explanation is that the relaxation time reflects the size of the spin textures, namely, larger spin textures fluctuate more slowly and have a longer life span and smaller ones have shorter lifetimes. As we discuss above, when decreasing temperature, the precedently emergent belt-like spin textures grow up and become denser, and then, they are combined antiparallel to each other along

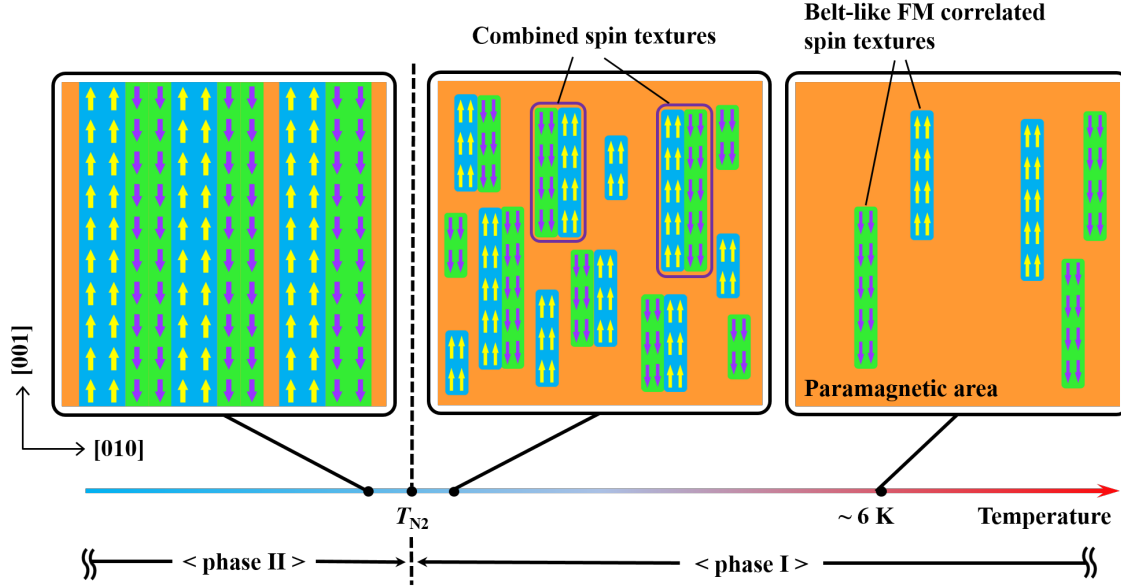


Figure 10: (Color online) Schematic picture of the ordering process of the I-II phase transition in the D_1 plane, which is represented by the column of the orange cross-squares surrounded by the green dashed rectangle in Fig. 2. All the panels show the projection of the D_1 plane onto the a -plane. The orange-shaded areas represent the region where the spins are fluctuating (noted as paramagnetic area) and the blue and green rectangles represent the “belt-like” FM spin textures whose spins are parallel and antiparallel with the c -axis. The purple rectangles in the middle panel represent the antiparallely combined belt-like spin textures.

the b -axis by the AFM NNN and further long-range interactions. It is schematically shown in the middle panel of Fig. 10 by the purple rectangle frame. Once they are combined, the spin textures are not FM but striped AFM, thus they no longer contribute to the response to the uniform ac field dominantly. On the other hand, the remaining small fragment of FM spin textures predominantly contribute to the ac response. As a result, the relaxation time of the dynamics measured by the ac susceptibility becomes shorter as approaching T_{N2} because the size of the FM spin textures predominantly responding to the ac field becomes smaller. That is to say, the non-thermally activated behavior of the ac response may indicate the shift of the spin correlations from the isolated FM spin textures to the striped AFM ones.

The fact that there is the temperature hysteresis over the I-II phase transition can be also explained. In this picture, the I-II phase transition is the spontaneous arrangement of the large belt-like FM spin textures. This ordering process should be extremely slower than conventional magnetic phase transitions because the time-scale of the dynamics of the units of the ordering, the belt-like FM spin textures, is very long, being the order of 10-100 ms. Thus, the temperature hysteresis should be observed in the conventional experimental time-scale (order of second or

minute). The details of the hysteresis behaviors observed in T_{χ_s} and τ_s are discussed below. As shown in Figs. 9 (c) and (b), T_{χ_s} in the heating process is larger than that in the cooling one, and τ_s in the heating process is shorter than that in the cooling one below T_{N2} and is longer above T_{N2} . In our scenario, these hysteresis behaviors can be interpreted as the difference between the “solidification” of the belt-like FM spin textures and “melting” of the striped order in the D_1 plane, which correspond to the cooling and heating processes, respectively. The former is the process described so far and the latter is the opposite process where the complete striped structure of the phase II breaks into the belt-like FM textures. Above T_{N2} , it is naturally expected that larger FM spin textures are more densely persist in the “melting” process and, vice versa, smaller spin textures should be frequently formed in the “solidification” process. Thus, the spin correlations T_{χ_s} should be larger on the heating process than those on the cooling one and the relaxation time τ_s in the heating process should be longer than that in the cooling process above T_{N2} . On the other hand, since the stable state is the stripe AFM below T_{N2} , the size relationship of the fragment of FM spin textures is reversed, namely, larger spin textures persist in the solidification process and vice versa. Thus, τ_s below T_{N2} should be longer in the cooling process

than that in the heating process.

At last, we discuss the question that the novel slow critical dynamics is only present in the I-II phase transition but is absent in the para-I phase transition at T_{N1} . Probably, this comes from the difference between the dimensionality of these two phase transitions. As we mentioned in Sec. 1, paramagnetic spins in the D_I plane can be considered as a pseudo two-dimensional system. The I-II phase transition is the process where the fluctuating spins in these D_I planes order into the striped structure. On the other hand, the para-I phase transition is the process where the fluctuating spins in the three-dimensional paramagnetic state order. In general, low dimensionality enhances the fluctuations and destabilizes the ordered state in the system. The extraordinary ordering process of the I-II phase transition, namely, the precedent emergence of the large spin textures and their spontaneous arrangement can be a consequence of its low dimensionality.

6 Summary

We performed the ac susceptibility measurements of the frustrated magnet $DyRu_2Si_2$, especially in the vicinity of the phase transition between the partially ordered phases I and II. Detailed analysis of the temperature and frequency dependences of the ac susceptibility reveals the novel critical dynamics of the I-II phase transition. The temperature dependences of the relaxation time and isothermal susceptibility indicate the following three striking features. First, the dynamic FM correlations with extremely long relaxation time appear precedently at around 6.0 K and grow towards the phase transition temperature T_{N2} . Second, the dynamic FM correlations exhibit non-thermally activated behavior. Third, the dynamics shows the hysteresis behavior. On the basis of these features, we propose the process of this phase transition as shortly described as follows. In the D_I plane, which is the emergent two-dimensional disordered system in the phase I, the large and stable belt-like FM spin textures formed by the NN FM interactions appear as precursors around 6.0 K. With decreasing temperature towards T_{N2} , they become denser, more likely to come next to each other along the b-axis and combined when they are antiparallel to each other due to the NNN AFM and further long-range interactions. Eventually, they spontaneously form the striped structure of the phase II at T_{N2} .

We will perform the neutron scattering experiments in the near future to verify our hypothesis about the ordering process of the I-II phase transition. We expect to observe the development and shift of the spin

correlations from the broad FM correlations to the sharp stripe ones around $(2/9, 2/9, 0)$ in the reciprocal lattice space, which substantially verifies our hypothesis on the spin ordering in the pseudo two-dimensional plane.

Acknowledgements

The authors acknowledge the support from the JSPS Grant-in-Aid for Scientific Research (B) (No. 20H01852).

References

- [1] D. Hüser, L. E. Wenger, A. J. van Duynveldt, and J. A. Mydosh, *Phys. Rev. B* **27**, 3100(R) (1983).
- [2] K. Gunnarsson, P. Svedlindh, P. Nordblad, L. Lundgren, H. Aruga, and A. Ito, *Phys. Rev. Lett.* **61**, 754 (1988).
- [3] P. Granberg, L. Sandlund, P. Nordblad, P. Svedlindh, and L. Lundgren, *Phys. Rev. B* **38**, 7097 (1988).
- [4] K. Jonason, E. Vincent, J. Hammann, J. P. Bouchaud, and P. Nordblad, *Phys. Rev. Lett.* **81**, 3243 (1998).
- [5] J. A. Quilliam, L. R. Yaraskavitch, H. A. Dabkowska, B. D. Gaulin, and J. B. Kycia, *Phys. Rev. B* **83**, 094424 (2011).
- [6] H. Takatsu, K. Goto, T. J. Sato, J. W. Lynn, K. Matsubayashi, Y. Uwatoko, R. Higashinaka, K. Matsuhira, Z. Hiroi, and H. Kadowaki, *J. Phys. Soc. Jpn.* **90**, 123705 (2021).
- [7] K. Matsuhira, Y. Hinatsu, and T. Sakakibara, *J. Phys.: Condens. Matter.* **13**, L737 (2001).
- [8] J. Flouquet, S. Kambe, L. P. Regnault, P. Haen, J. P. Brison, F. Lapiere, and P. Lejay, *Physica B* **215**, 77 (1995).
- [9] T. Shigeoka, N. Iwata, and H. Fujii, *J. Magn. Magn. Mater.* **104-107**, 1229 (1992).
- [10] M. S. da Silva, J. B. Sousa, B. Chevalier and J. Étourneau, *J. Appl. Phys.* **76**, 6344 (1994).
- [11] A. Garnier, D. Gignoux, B. Ouladdiaf, D. Schmitt and T. Shigeoka, *Physica B* **254**, 166 (1998).
- [12] B. Andreani, G. L. F. Fraga, A. Garnier, D. Gignoux, D. Maurin, D. Schmitt, and T. Shigeoka, *J. Phys.: Condens. Matter.* **7**, 1889 (1995).

- [13] S. Kawano, M. Takahashi, T. Shigeoka, N. Iwata, M.J. Bull, *Physica B* **346-347**, 99 (2004).
- [14] A. Dönni, G. Ehlers, H. Maletta, P. Fischer, H. Kitazawa, and M. Zolliker, *J. Phys.: Condens. Matter.* **8**, 11213 (1996).
- [15] Z. Fu, Y. Zheng, Y. Xiao, S. Bedanta, A. Senyshyn, G. G. Simeoni, Y. Su, U. Rücker, P. Kögerler, and T. Brückel, *Phys. Rev. B* **87**, 214406 (2013).
- [16] B. Yan, A. K. Paul, S. Kanungo, M. Reehuis, A. Hoser, D. M. Többens, W. Schnelle, R. C. Williams, T. Lancaster, F. Xiao, J. S. Möller, S. J. Blundell, W. Hayes, C. Felser, and M. Jansen, *Phys. Rev. Lett.* **112**, 147202 (2014).
- [17] O. A. Petrenko, M. R. Lees, G. Balakrishnan, and D. McK Paul, *Phys. Rev. B* **70**, 012402 (2004).
- [18] J. A. M. Paddison, G. Ehlers, A. B. Cairns, J. S. Gardner, O. A. Petrenko, N. P. Butch, D. D. Khalyavin, P. Manuel, H. E. Fischer, H. Zhou, A. L. Goodwin, and J. R. Stewart, *npj Quantum Mater.* **6**, 99 (2021).
- [19] J. D. M. Champion, A. S. Wills, T. Fennell, S. T. Bramwell, J. S. Gardner, and M. A. Green, *Phys. Rev. B* **64**, 140407(R) (2001).
- [20] J. R. Stewart, G. Ehlers, A. S. Wills, S. T. Bramwell, and J. S. Gardner, *J. Phys.: Condens. Matter.* **16**, L321 (2004).
- [21] S. A. M. Mentink, A. Drost, G. J. Nieuwenhuys, E. Frikkee, A. A. Menovsky, and J. A. Mydosh, *Phys. Rev. Lett.* **73**, 1031 (1994).
- [22] A. Zorko, M. Pregelj, M. Klanjšek, M. Gomilšek, Z. Jagličić, J. S. Lord, J. A. T. Verezhak, T. Shang, W. Sun, and J.-X. Mi, *Phys. Rev. B* **99**, 214441 (2019).